NISTIR 6024

Evaluation of Press-and-Sinter Parameters for Tantalum Pentoxide by the Diametral Compression Test

Prepared by:

Z. Livne
Nuclear Research Center Negev
Beer-Sheva, Israel

R. J. Fields
U.S. Department of Commerce
Metallurgy Division
National Institute of Standards
and Technology
Gaithersburg, Maryland 20899

A. Agulyansky
TAN Ceramics Ltd.
Tel-Aviv, 61116, Israel

NIST

NISTIR 6024

Evaluation of Press-and-Sinter Parameters for Tantalum Pentoxide by the Diametral Compression Test

Prepared by:

Z. Livne
Nuclear Research Center Negev
Beer-Sheva, Israel

R. J. Fields
U.S. Department of Commerce
Metallurgy Division
National Institute of Standards
and Technology
Gaithersburg, Maryland 20899

A. Agulyansky
TAN Ceramics Ltd.
Tel-Aviv, 61116, Israel

May 15, 1997

U.S. DEPARTMENT OF COMMERCE
William M. Daley, Secretary

TECHNOLOGY ADMINISTRATION
Gary R. Bachula, Acting Under Secretary
for Technology

NATIONAL INSTITUTE OF STANDARDS
AND TECHNOLOGY
Raymond G. Kammer, Director

EVALUATION OF PRESS-AND-SINTER PARAMETERS FOR Ta_2O_5 BY THE DIAMETRAL COMPRESSION TEST

Z. Livne[1] and R. J. Fields
Metallurgy Division
National Institute of Standards and Technology
Gaithersburg, Maryland 20899

A. Agulyansky
TAN Ceramics Ltd.
Tel-Aviv 61116 ISRAEL

Abstract

Submicron Ta_2O_5 powder was consolidated by cold pressing using pressures between 24 MPa and 240 MPa followed by sintering at temperatures in the range 1300 °C to 1500 °C. The resulting disks were fractured in diametral compression tests (DCT) to determine the tensile strength. The strength, mode of fracture, and fracture surface were subsequently used to identify potential processing routes for high density, fine grained Ta_2O_5 for use as sputtering targets. Besides the conventional single or triple cleft fracture, two other modes of failure were observed in the diametral compression test: **delamination** due to stratification flaws introduced by high pressure pre-pressing before sintering, and **fragmentation** caused by slow microcrack growth in the presence of phase transformation stresses arising in samples sintered above the transformation temperature of 1360 °C. It is important to achieve a fine grain or particle size not only to optimize the sintering parameters, but also to withstand the phase transformation stresses that build up in this material on cooling. It also appears that the transformation stresses are less detrimental in porous samples because of the reduced constraint around each grain.

Introduction

Ta_2O_5 is an electronic material that has a useful combination of dielectric constant, temperature dependence of the dielectric constant, resistance to electric field breakdown, and electrical resistivity {1,2,3}. It is used as a thin film capacitive material in some applications where it is produced by sputtering {2,3}. The fabrication of mechanically sound sputtering targets of Ta_2O_5 is

---

[1] Guest scientist at the National Institute of Standards and Technology from 8/15/94-8/14/95. Now at the Nuclear Research Center, Negev, Israel.

difficult due to its crystalline anisotropy and the occurrence of a high temperature phase transformation {4}.

In recent years, considerable interest in nanocrystalline materials has developed due to the possibility that consolidation of the powder may be greatly improved due to the large surface area {5}. Furthermore, it is possible that the fine grain size would be beneficial in overcoming microcracking problems arising from the anisotropic expansion and phase transformation behavior {6}. Here, nanocrystalline Ta_2O_5 powder is consolidated by cold pressing and sintering under a variety of conditions. The strength of the resulting compacts are determined from diametral compression tests (DCT) {7}. The mode of fracture is also found to be extremely helpful in choosing an optimum processing route.

Experimental Procedure

Powder: The Ta_2O_5 powder used in the present study was prepared by TAN Ceramics Ltd[2]. It was prepared by a method based on liquid-liquid extraction. The method includes decomposition of low grade tantalum powder, purification of the solution by liquid-liquid extraction, precipitation and thermal treatment of tantalum hydroxide. The phase condition and purity of the Ta_2O_5 powder so obtained was studied by X-ray diffraction, X-ray fluorescence, and DC arc emission spectral techniques. The powder was found to be beta-Ta_2O_5 containing the following impurity contents in ppm:

Element	PPM	Element	PPM	Element	PPM
Al	4(6)	Mg	6(9)	Sn	3(4)
Ca	8(9)	Mn	<1(8)	Ti	<1(3)
Co	<1(9)	Nb	6(5)	V	2(4)
Cr	2(5)	Ni	2(6)	Zn	3(4)
Cu	<1(6)	Pb	3(4)	Zr	1(8)
Fe	<1(2)	Si	<1(8)	Mo	<1(3)

where the number in parentheses is the relative standard deviation of the measurement. The particle diameter was measured by a light scattering method and found to have an average value of 417 nanometers with a standard deviation of 196 nanometers. Microscopic examination revealed powder particles that were short rods with a typical diameter of 0.2 micrometer to 1 micrometer and a typical length to diameter ratio of 2 to 2.5 (Fig 1).

Cold Pressing: Cold pressing was accomplished in a standard piston cylinder die having an inside diameter of 10 mm. The procedure for producing the green tablets was to place

---

[2] Identification of the source of the Ta_2O_5 powder is provided only to better define the experimental conditions and is not intended as an endorsement.

approximately 1 gram of powder in the die, insert the piston, and press. The pressures used were 24 MPa (240 atm), 80 MPa (800 atm), 160 MPa (1600 atm), and 240 MPa (2400 atm). The green density of the resulting tablets varied from 48% of theoretically fully dense at 24 MPa to 58% at 240 MPa.

Sintering: For each level of pressing, three sintering temperatures (1300, 1400, and 1500 °C) and five sintering times (1, 2, 3, 5, 8 hours) were investigated. Sintering was carried out in air at atmospheric pressure.

Characterization: Only one sample per condition was studied. While this led to greater variablity in results, it permitted a larger number of conditions to be investigated. Since processing trends were the goal, this source of error was accepted as the best compromise given the amount of material available.

The densities of the green and sintered bodies were determined by weighing, and, by measuring the dimensions of the tablets which were disks having nominal dimensions of 10 mm diameter and 3 mm thick, calculating the volume. This method of determining density has an error of about 0.05 g/mL.

The strength after sintering was evaluated by the diametral compression test, DCT. The DCT has been described and analyzed in a detailed paper by Rudnick et al. {7}. The test is an experimentally simple method for measuring the tensile strength in brittle materials. A right circular cylindrical specimen is compressed diametrically between two flat platens as shown in Fig.2. The maximum tensile stress, σ_{max}, develops normal to the loading diameter and in direct proportion to the applied load, P:

$$\sigma_{max} = 2P/\pi Dt \qquad (1)$$

where D and t are the cylinder's diameter and thickness. The tensile stress causes the cylinder to fracture along the diametral plane joining the lines of contact of the specimen and the platens. Failure in the DCT usually occurs as either a single fracture or a "triple-cleft", in which the specimen breaks into four pieces. Fractography was carried out on the broken pieces in the scanning electron microscope as the final type of characterization.

Results

The effect of different cold pressing pressures, sintering times, and sintering temperatures on the resulting densities are shown in Fig. 3. The relative density indicated on the figure is the actual density normalized by the theoretically fully dense value of 8.735 g/mL for Ta_2O_5. The green density at the start of all the sintering studies increases with initial cold pressing pressure. At 1300 °C, the density increases nearly linearly with time for all cold pressing pressures. At 1400 °C, a plateau in density with increasing sintering time is observed for all cold

pressing pressures except the lowest. In this case, sintering continues and produces the densest compact obtained in the present study. At 1500 C, a rapid densification from the green state is observed in the first hour, followed by a virtually unchanging or even decreasing density with increasing time after that. No cross-over in density was observed at 1300 °C or 1500 °C similar to the cross-over that occurred at 1400 °C.

The effect of different cold pressing pressures, sintering times, and sintering temperatures on the resulting fracture behavior are shown in Fig. 4a-c. The two expected modes of fracture, i.e., diametral splitting and triple-cleft (Fig. 5a), were observed in high load fractures. In addition, two other modes were found to result in extremely low load failures. A crushing type of failure broke the tablet into small fragments as seen, for example, in Fig. 5b. The other mode resulted in a delamination in a plane normal to the longitudinal axis of the disk shaped test specimens. This left two disks of decreased thickness as the fracture product as seen in of Fig. 5c. Sometimes these two disks then broke by normal splitting or triple-cleft, but at a greatly reduced load compared to specimens that had not split longitudinally. The breaking loads for each processing schedule are given in Table 1. The maximum tensile strengths were determined using Eqn. 1 for all fractures and are also listed in Table 1. While there is some variability, most of the specimens heated at 1300 °C broke by normal splitting or triple-cleft in a load range of 100 to 400 N. A few, prepressed at 160 and 240 MPa exhibited longitudinal splitting and failed at a low load. In general, the results at 1400 °C were similar to those at 1300 °C, but with slightly lower loads. In contrast, many samples heated at 1500 °C failed by crushing into small fragments at nearly zero load. This was especially true of samples prepressed at 160 and 240 MPa. Even the few samples which broke normally, failed at very low loads compared to those sintered at lower temperatures. Load versus displacement curves typical of the three fracture modes are shown in Fig 6a-c. The conventional single or triple cleft fracture is by far the strongest mode and occurs when processing defects have not significantly weakened the material.

In Fig. 7, the external surfaces of tablets sintered at 1300, 1400, and 1500 °C are shown, giving some idea of the grain coarsening that takes place at the various sintering temperatures. Note that, even after only 3 hours at 1300 °C, the grains are about 1 μm in diameter (Fig. 7a). Furthermore, while the samples heated at 1300 and 1400 °C seem to be fairly dense and well bonded, that at 1500 °C (Fig. 7c) has large pores and peculiar necks formed between particles. This microstructure is typical of coarsening without shrinkage {8}. In Fig. 8 and 9, fractographs allow internal characterization. In the case of Fig. 8, the fractographs are of the typical diametral splitting fracture surface, i.e. an internal surface parallel to the longitudinal axis. The fracture surfaces of samples sintered at 1300 and 1400 °C (Fig. 8a and b) suggest that most of the grains were well bonded to their neighbors over a significant portion of their grain boundary area. In

contrast, the sample at 1500 °C (Fig. 8c) had numerous cracks and bonds between neighboring grains occurred to a much lesser extent than in the other samples. In Fig. 9, the fracture surface of a longitudinal split (Fig 9a), i.e. an internal surface perpendicular to the longitudinal axis, is compared with that of a diametral split that occurred in the same sample (Fig 9b). The longitudinal split shows practically no evidence of bonding between the two surfaces, suggesting that this flaw existed before sintering. Clearly, as seen in the fractograph of the diametral split, regions that were in contact prior to sintering were well bonded in this sample.

Discussion

One of the primary goals of powder consolidation is to achieve dense, pore-free bodies. In some cases it is not necessary to reach theoretical full density, but usually it is desirable to eliminate interconnected porosity. Interconnected porosity begins to disappear at relative densities of 85 to 90%. Considering this goal, it is apparent that heating at 1500 °C is not desirable as no combination of cold pressing pressure or time-at-temperature could achieve much more than 80% relative density in Ta_2O_5 at this temperature. None of the conditions investigated at a sintering temperature of 1300 C gave densities much more than 80% either, but the trend of the density-time curves in Fig. 3a suggest that continued heating beyond 8 hours might result in densities high enough to assure an absence of interconnected porosity. In contrast, sintering of Ta_2O_5 powder at 1400 °C resulted in numerous instances of densities above 85% in the times investigated here. The behavior of the specimen cold pressed to only 24 MPa and sintered at 1400 °C was intriguing. Not only was it the densest material after 8 hours of sintering, but it also showed no sign of a plateau in density with sintering time.

Another goal of powder consolidation is to achieve a body with a certain minimum strength. Using the DCT it was possible to determine the tensile strength of samples which broke either by diametral splitting or triple-cleft. Many processing routes at sintering temperatures of 1300 or 1400 °C were identified that gave reasonable tensile strengths for a sputtering target. If another mode of failure appeared, a processing defect should be suspected as the cause of low load fracture. The longitudinal splitting that was observed in 160 to 240 MPa prepressed powder sintered at 1300 or 1400 °C is most likely due to the stratification or layering that occurs during high pressure unidirectional pressing in a die. It results from friction between the powder and the die wall. The fractography in Fig. 9 supports the idea that an internal surface, i.e. a flaw, existed prior to sintering and was responsible for the longitudinal splitting.

The crushing mode of failure that only occurred at a sintering temperature of 1500 °C may be due to the fact that there is a phase transformation in Ta_2O_5 {2}. It is well known that phase

transformations cause internal stresses leading to microcracks that greatly reduce the strength. Evidence of such cracking may be visible in Fig. 8c. The fact that spontaneous failure was observed during storage suggests that slow crack growth takes place in this material resulting in various amounts of damage. While the transformation in Ta_2O_5 is reported to occur at 1360 °C, it depends on purity and may be different for the material used in this study, thus explaining the fact that only the material sintered at 1500 °C seemed to suffer transformation cracking. Alternately, it is possible that the fine grain size retained at 1400 °C was able to minimize the effects of the phase transformation. Besides the large grains in the 1500 °C material, the peculiar necks which formed and the high porosity, both reducing the area of contact between grains, contribute to the observed weakness.

At 1300 °C, longer sintering times lead to denser and stronger material. At 1400 °C, longer sintering times lead to denser and weaker material. A possible explanation for this is that the lack of constraint around grains in the porous condition permits the transformation to occur without building up detrimental residual stresses. At 1500 °C, longer sintering times lead to weaker material, but this is due to grain growth as there is no densification with time at this temperature.

Conclusion

The consolidation of submicron Ta_2O_5 powder by cold pressing and sintering was studied. It was found that high, cold pressing pressures of 160 MPa to 240 MPa generated longitudinal defects in disk shaped samples that ultimately resulted in longitudinal splitting. It was also found that sintering at 1500 °C caused microcracking and coarsening without densification, resulting in very weak and porous bodies. While sintering at 1300 °C produced strong samples, it did not result in densities greater than 80% even after 8 hours of sintering. The best combination of strength and density was found in samples that had been cold pressed at moderate to low pressures of 24 MPa to 80 MPa and sintered at 1400 °C for several hours.

Under these optimized conditions, the significant grain growth occurs. Although not studied here, a sintering temperature just below the transformation temperature (e.g., 1350 °C) would probably be beneficial. Also, a starting powder having a finer grain or particle size would probably improve consolidation and retain its fineness after sintering at such a temperature. The fine grain size would reduce the intergrain stress levels arising from thermal expansion anisotropy and increase the ability of the material to support applied loads. There would be no need for porosity to mitigate transformation induced stresses.

The crushing of the samples into small fragments that was observed to occur at virtually zero applied load is most likely caused by internal stresses or microcracks arising from the volume change of the grains due to the phase transformation. Again, the

level of these internal stresses and the durability of the sintered material may be improved by using powder with much smaller grain or particle size than was consolidated here.

The diametral compression test was found to be an extremely useful tool in the present study. Sample preparation and test performance were simple and straight forward. The data was consistent and provided a good idea of the tensile strength of the material. Lastly, the DCT provided a clear means to distinguish between different processing defects that caused reductions in strength and early failure.

Acknowledgements

The authors would like to thank Dr. R. B. Clough for assistance in performing the mechanical testing and Dr. R. S. Roth for advice and helpful discussions on the phase transformation in Ta_2O_5.

References

1. W. S. Lau, T. S. Tan, N. P. Sandler, and B. S. Page, "Characterization of Defect States Responsible for Leakage Current in Tantalum Pentoxide Films for Very-High-Density Dynamic Random Access Memory (DRAM) Applications," Japanese Journal of Applied Physics **34**, 757-(1995).

2. H. Shinriki, T. Kisu, S.-I. Kimura, Y. Nishioka, Y. Kawamoto, and K. Mukai, " Promising Storage Capacitor Structures with Thin Ta_2O_5 Film for Low-Power High-Density DRAM's," IEEE Transactions on Electron Devices **37**, 1939-1946 (1990).

3. K. Ohta, K. Yamada, K. Shimizu, and Y. Tarui, "Quadruply Self-Aligned Stacked High-Capacitance RAM Using Ta_2O_5 High-Density VLSI Dynamic Memory," IEEE Transactions on Electron Devices **29**, 368-376 (1982).

4. N. C. Stephenson and R. S. Roth, "The Crystal Structure of the High Temperature Form of Ta_2O_5," J. of Solid State Chemistry **3**, 145-153 (1971).

5. G.P. Dransfield, P. McColgan, I. Birkby, J.R.G. Evans, and J. H. Song, "The Manufacture of Ceramic Components from Ultrafine Oxide Powders," in Nanoceramics, edited by R. Freer, published by The Institute of Materials, London (1993) pp. 15-23.

6. A. G. Evans, "Microfracture from Thermal Expansion Anisotropy -- I. Single Phase Systems," Acta Metallurgica 26, 1845-1853 (1978).

7. A. Rudnick, A. R. Hunter, and F. C. Holden, "An Analysis of the Diametral-Compression Test," Materials Research and Standards **3**, 283-289 (1963).

8. W. D. Kingery and B. Francois, "The Sintering of Crystalline Oxides, I. Interactions between Grain Boundaries and Pores," in Sintering and Related Phenomena, edited by G. C. Kuczynski, N. A. Hooten, and C. F. Gibbon, published by Gordon and Breach, New York (1967) pp. 471-499.

Figure Captions

Figure 1. Scanning electron micrographs of Ta_2O_5 powder, a) x2500 b) x10,000.

Figure 2. Compressive force, P, applied as shown generates a fairly uniform tensile stress on a diametral plane. Stress distribution from Ref. 4.

Figure 3. Density resulting from different cold pressing pressures, sintering times, and sintering temperatures, a) 1300 °C, b) 1400 °C, and c) 1500 °C.

Figure 4. Fracture behavior resulting from the different press-and-sinter parameters, a) 1300 °C, 1400 °C, and 1500 °C.

Figure 5. Different modes of fracture in the diametral compression test, a) triple cleft fracture, b) fragmentation, and c) separation along a plane perpendicular to the longitudinal axis of the disk (longitudinal delamination).

Figure 6. Load versus displacement curves typical of the three fracture modes, a) single or triple-cleft fracture, b) crushing type of fracture (fragmentation), and c) delamination failure.

Figure 7. External surfaces of tablets prepressed at 24 MPa and sintered for 3 hours at a) 1300 °C, b) 1400 °C, and c) 1500 °C.

Figure 8. Diametral splitting fracture surfaces of tablets prepressed at 24 MPa and sintered for 3 hours at a) 1300°C, b) 1400 °C, and c) 1500 °C. All at X10,000.

Figure 9. Fractography of sample prepressed at 240 MPa and sintered at 1400 °C for 3 hours. a) Fracture surface of a longitudinal split. b) Diametral split fracture surface of same sample.

Table 1. Fracture behavior of Ta_2O_5 consolidated at 1300 °C.

Cold Pressure (MPa)	Sinter Time (hr)	Max. Load (N)	Strength (MPa)	Fracture Mode*
24	1	95 ± 2	6.33 ± .13	TC
	2	27 ± 1	1.80 ± .07	"
	3	178 ± 2	11.87 ± .13	"
	5	115 ± 2	7.67 ± .13	DS
	8	157 ± 2	10.47 ± .13	TC
80	1	113 ± 2	7.53 ± .13	TC
	2	129 ± 2	8.60 ± .13	TC
	3	181 ± 2	12.07 ± .13	"
	5	199 ± 2	13.27 ± .13	Mixed: TC+DS
	8	260 ± 2	17.33 ± .13	TC
160	1	180 ± 2	12.00 ± .13	LS
	2	142 ± 2	9.47 ± .13	LS
	3	36 ± 1	2.40 ± .07	LS
	5	14 ± 1	0.93 ± .07	"
	8	57 ± 1	3.80 ± .07	Mixed: LS+DS
240	1	6 ± 1	0.40 ± .07	LS
	2	16 ± 1	1.07 ± .07	"
	3	41 ± 1	2.73 ± .07	"
	5	25 ± 1	1.67 ± .07	"
	8	387 ± 2	25.80 ± .13	TC

* TC is triple cleft, DS diametral split, and LS longitudinal split.

Table 1. (cont.) Fracture behavior of Ta_2O_5 consolidated at 1400 °C.

Cold Pressure (MPa)	Sinter Time (hr)	Max. Load (N)	Strength (MPa)	Fracture Mode*
24	1	282 ± 2	18.80 ± .13	TC
	2	105± 1	7.00 ± .07	TC
	3	172 ± 2	11.50 ± .13	TC
	5	59 ± 2	3.90 ± .13	DS
	8	62 ± 2	4.10 ± .13	"
80	1	350 ± 2	23.30 ± .13	TC
	2	72 ± 2	4.80 ± .13	"
	3	173 ± 2	11.50 ± .13	TC
	5	66 ± 2	4.40 ± .13	DS
	8	46 ± 2	3.10 ± .13	"
160	1	72 ± 2	4.80 ± .13	Mixed: LS+DS
	2	29 ± 2	1.93 ± .13	"
	3	60 ± 1	4.00 ± .07	"
	5	28 ± 1	1.87 ± .07	"
	8	64 ± 1	4.30 ± .07	DS
240	1	10± 1	0.67 ± .07	Mixed: LS+DS
	2	8 ± 1	0.53 ± .07	LS
	3	18 ± 1	1.20 ± .07	"
	5	25 ± 1	1.67 ± .07	Mixed: LS+DS
	8	0	0	LS

* TC is triple cleft, DS diametral split, and LS longitudinal split.

Table 1. (cont.) Fracture behavior of Ta_2O_5 consolidated at 1500 °C.

Cold Pressure (MPa)	Sinter Time (hr)	Max. Load (N)	Strength (MPa)	Fracture Mode*
24	1	27 ± 1	1.80 ± .07	Mixed: C+DS
	2	--	--	--
	3	43 ± 1	2.87 ± .07	Mixed: C+DS
	5	29 ± 1	1.93 ± .07	"
	8	37 ± 1	2.47 ± .07	"
80	1	18 ± 1	1.2 ± .07	Mixed: C+DS
	2	--	--	--
	3	0	0	Mixed: C+DS
	5	0	0	C
	8	23 ± 1	1.53 ± .07	DS
160	1	0	0	C
	2	0	0	"
	3	0	0	DS
	5	0	0	"
	8	0	0	DS
240	1	0	0	C
	2	0	0	"
	3	0	0	"
	5	0	0	"
	8	0	0	"

* TC is triple cleft, DS diametral split, LS longitudinal split, and C crushed into small fragments.
-- Not tested.

a.

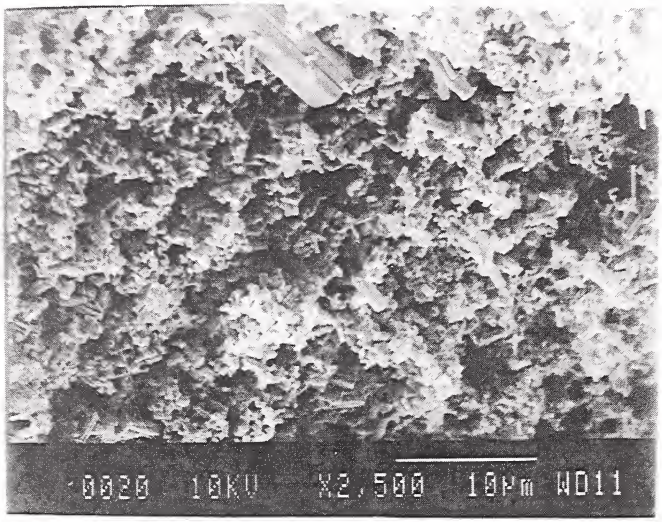

b.

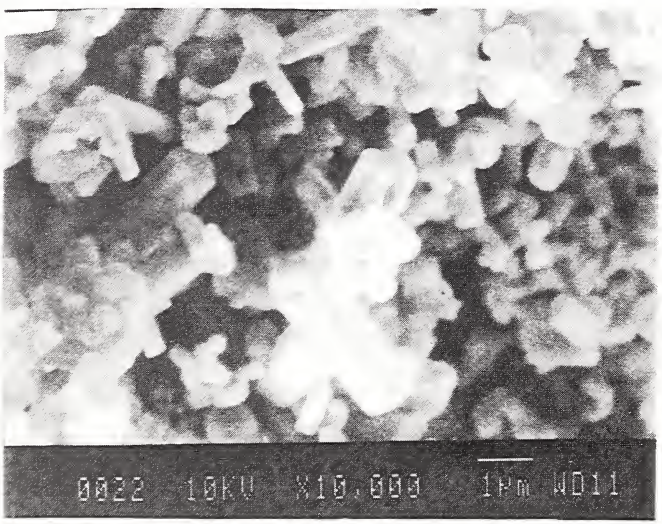

Figure 1. Scanning electron micrographs of Ta_2O_5 powder.
a.) X 2500 b.) X 10,000

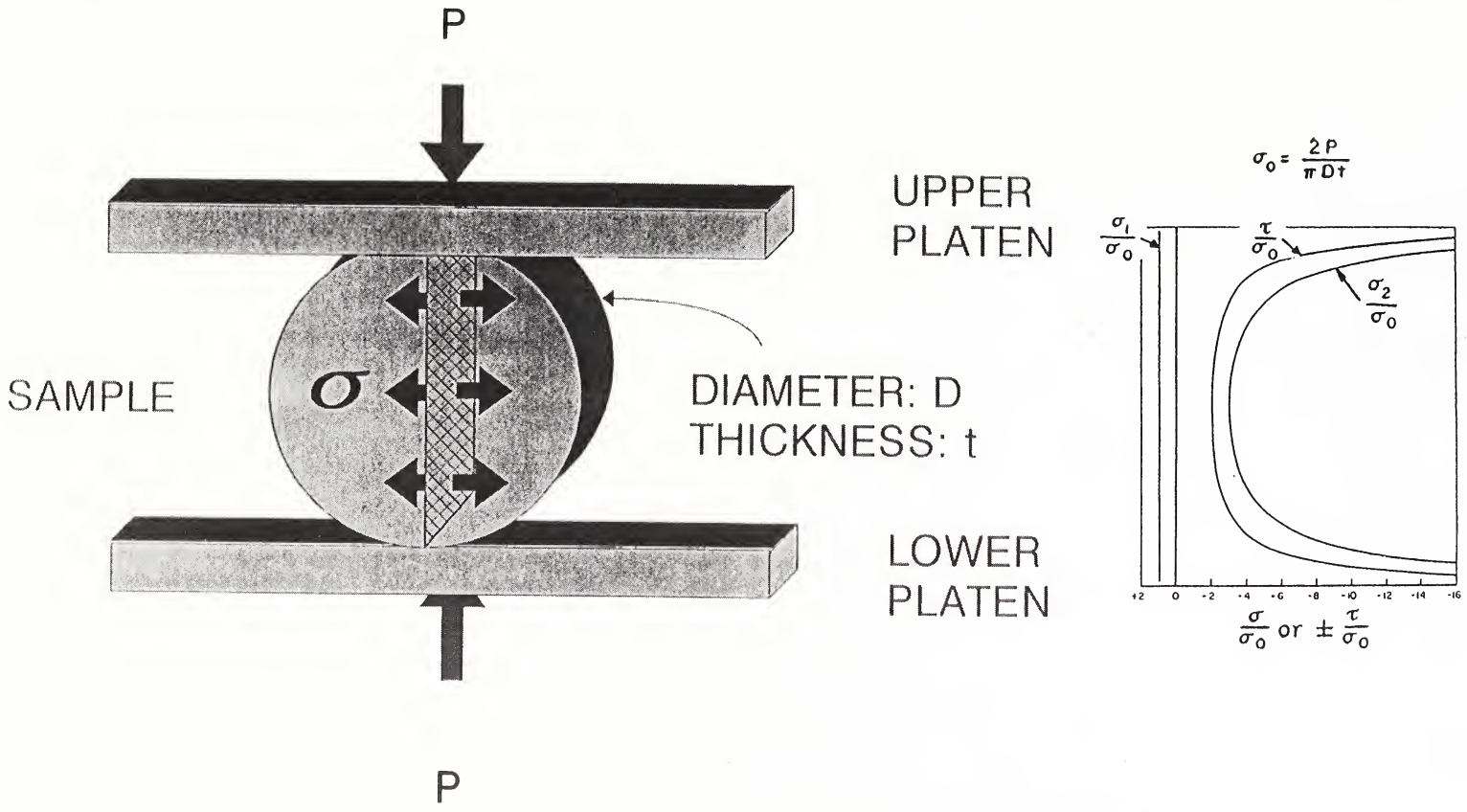

Figure 2. Compressive force, P, applied as shown generates a fairly uniform tensile stress on a diametral plane. Stress distribution along centerline is from Ref. 4.

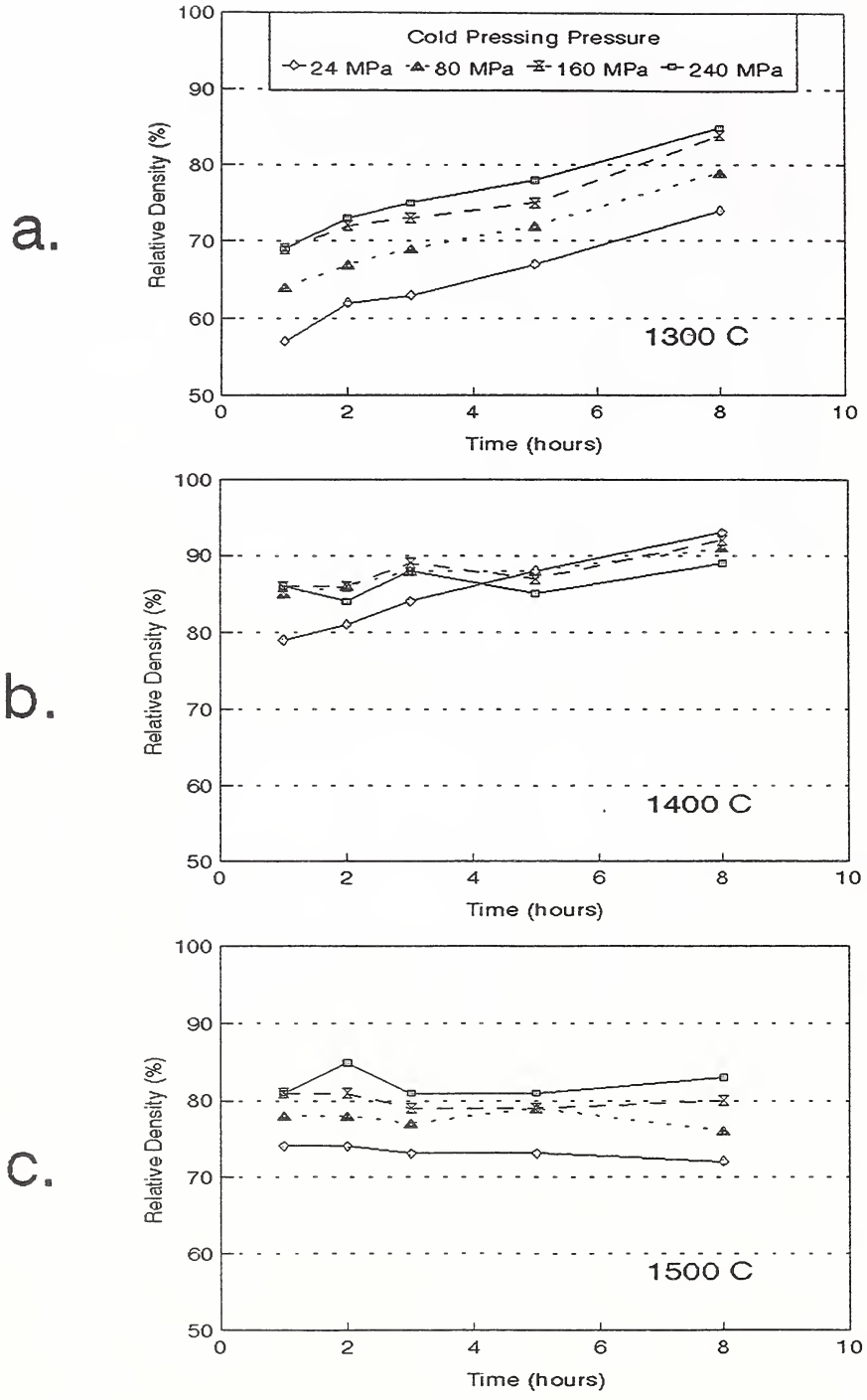

Figure 3. Density resulting from different cold pressing pressures, sintering times, and sintering temperatures: a) 1300, b) 1400, c) 1500 °C.

a.

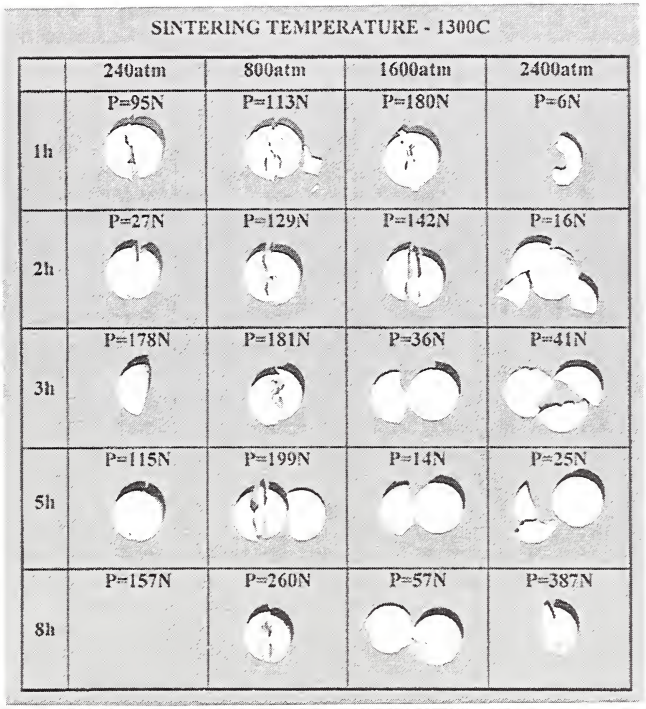

b.

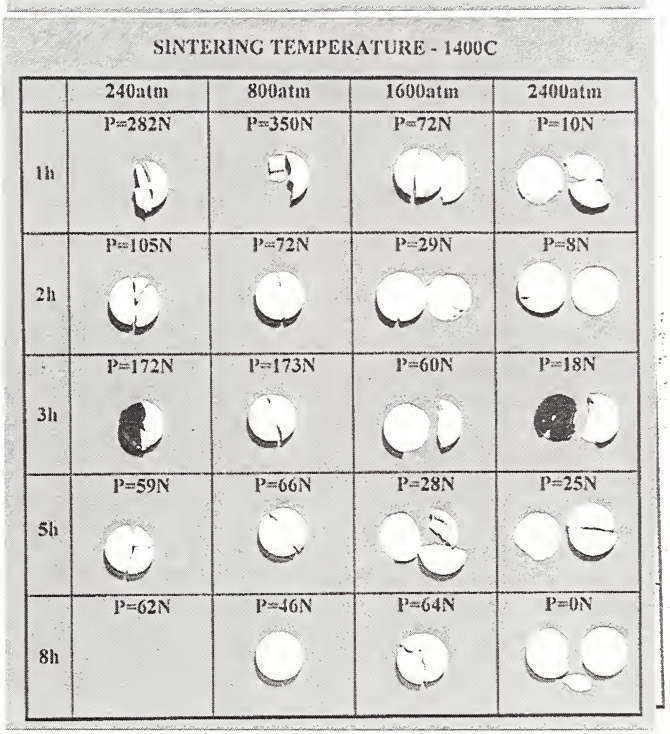

Figure 4. Fracture behavior resulting from the different press-and-sinter parameters: a) 1300 °C and b) 1400 °C.

c.

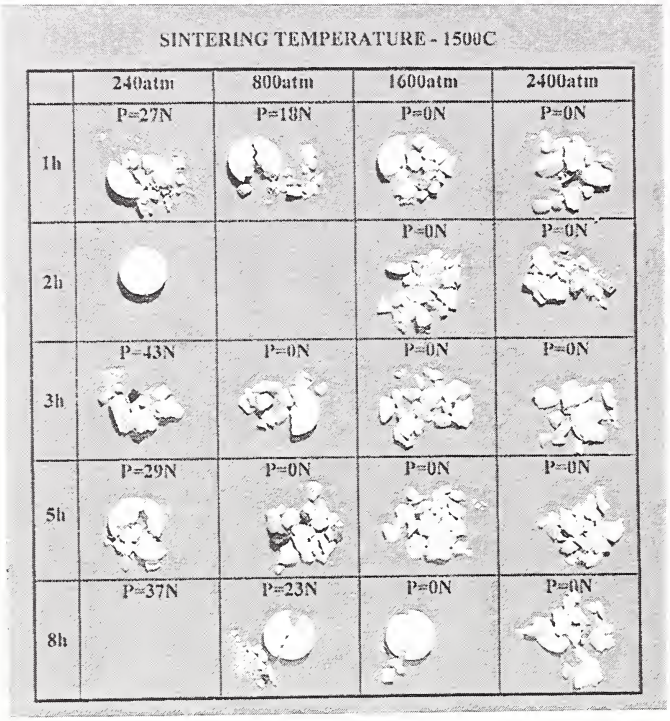

Figure 4.(cont.) Fracture behavior resulting from the different press-and-sinter parameters: c) 1500 °C.

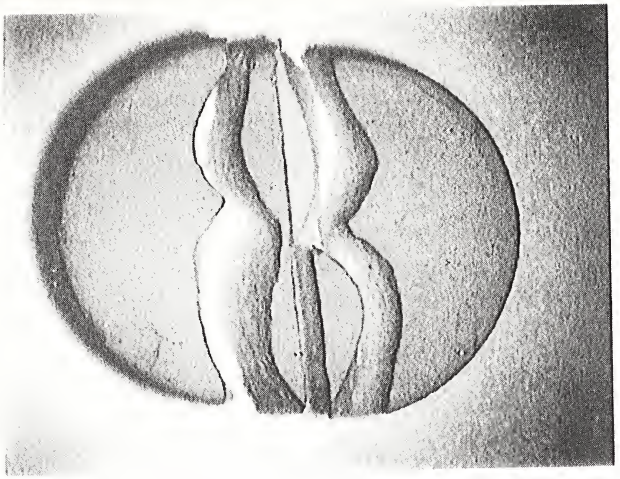

Mode I - Triple-cleft fracture

a.) Triple-cleft fracture, X6.

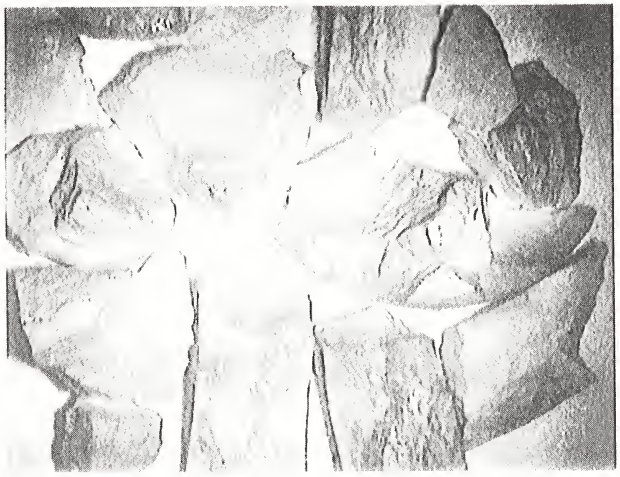

Mode III - Transform to small particles

b.) Fragmentation failure, X6.

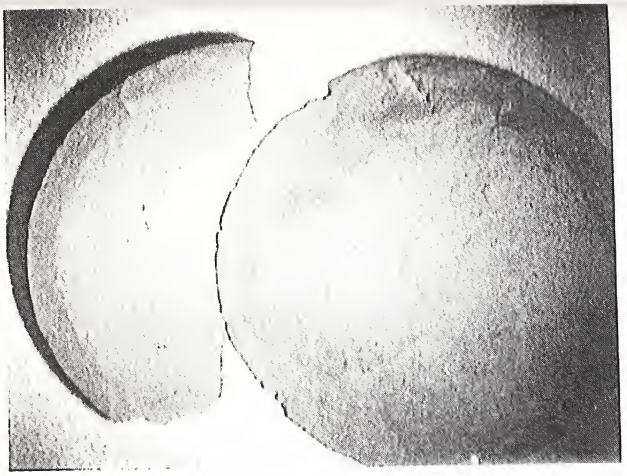

Mode II - Separation along a plane parallel to the flat sides of the pills

c.) Delamination failure, X6.

Figure 5. Different modes of fracture in the diametral compression test: a) triple cleft fracture, b.) fragmentation, and c.) separation along a plane perpendicular to the longitudinal axis of the disk (longitudinal delamination).

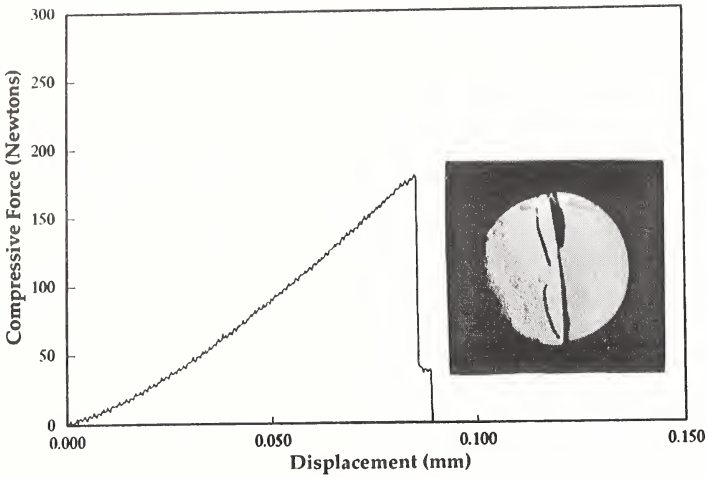

a) Triple-cleft fracture of sample prepressed at 24 MPa then sintered at 1300 °C for 3 hours (24MPa/3h/1300C).

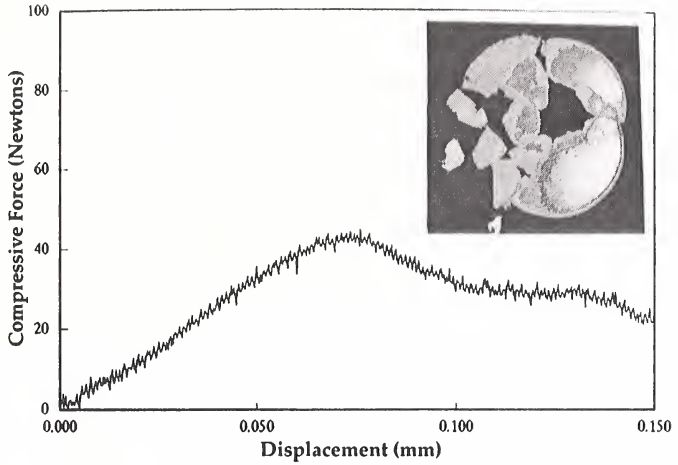

b) Fragmentation of sample (24MPa/3h/1500C).

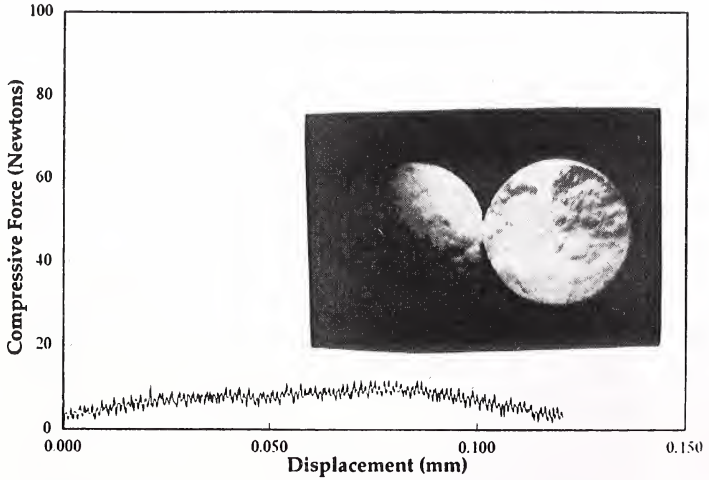

c) Delamination of sample (240MPa/2h/1400C).

Figure 6. Load versus displacement curves typical of the three fracture modes.

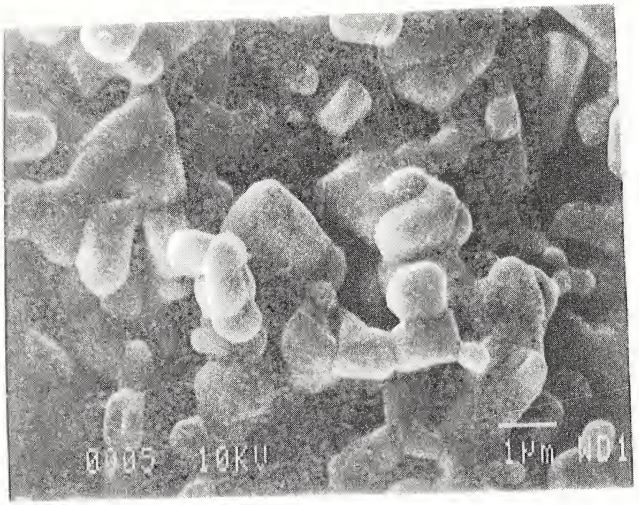

a.

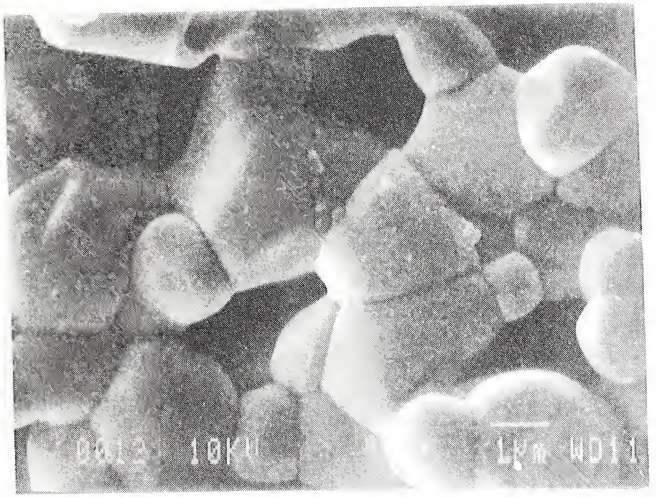

b.

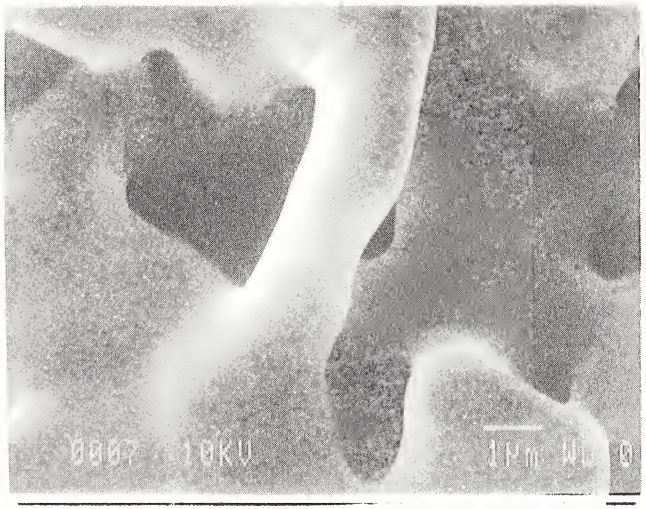

c.

Figure 7. External surfaces of tablets prepressed at 24 MPa and sintered for 3 hours at a) 1300 °C, b) 1400 °C, and c) 1500 °C.

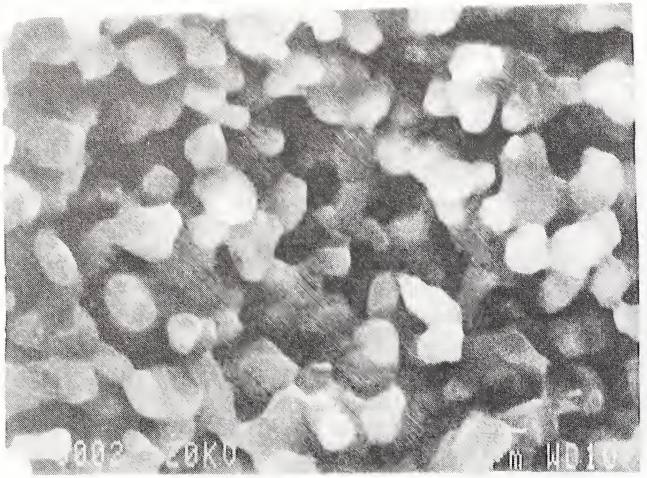

a.

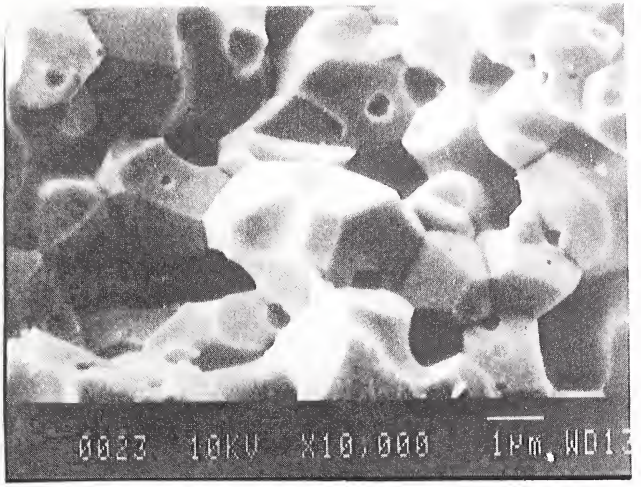

b.

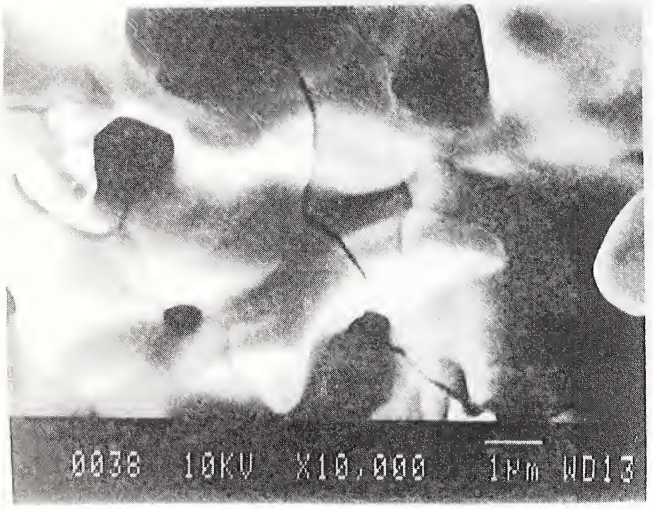

c.

Figure 8. Diametral splitting fracture surfaces of tablets prepressed at 24 MPa and sintered for 3 hours at a) 1300 °C, b) 1400 °C, and c) 1500 °C. (All X10,000).

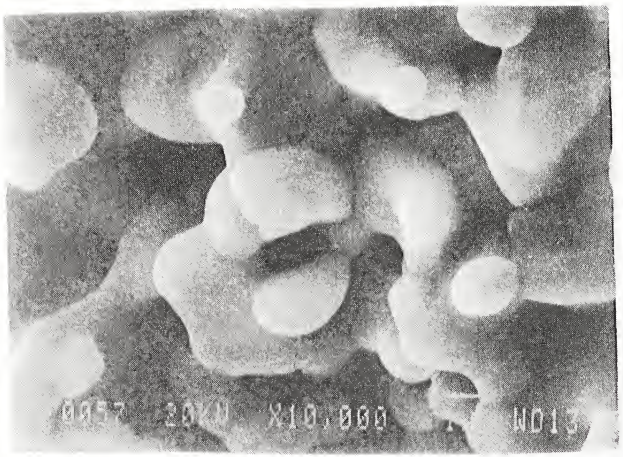

a.

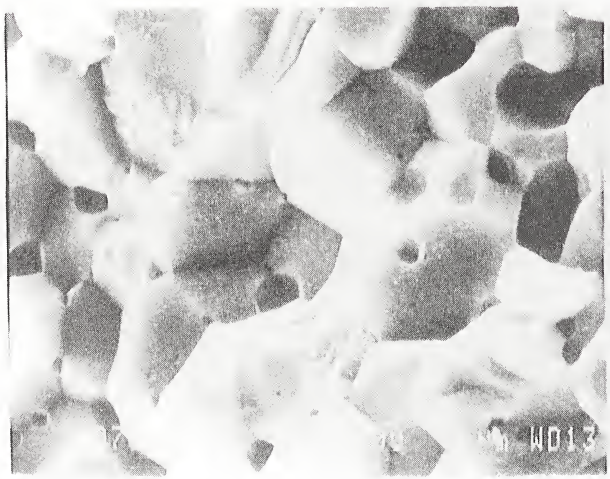

b.

Figure 9. Fractography of sample prepressed at 240 MPa and sintered at 1400 °C for 3 hours:
a) Fracture surface of a longitudinal delamination. (X10,000)
b) Diametral split fracture surface of same sample. (X10,000)